Eur. Phys. J. C (2025) 85:14
https://doi.org/10.1140/epjc/s10052-024-13717-2

THE EUROPEAN PHYSICAL JOURNAL C

Regular Article - Experimental Physics

Timing-based mass measurement of exotic long-lived particles at the FCC-ee

R. Aleksan[1], **E. Perez**[2], **G. Polesello**[3,a], **N. Valle**[3,b]

[1] IRFU, CEA, Université Paris-Saclay, 91191 Gif-sur-Yvette cedex, France
[2] CERN, Geneva, Switzerland
[3] INFN Sezione di Pavia, Via Bassi 6, 27100 Pavia, Italy

Received: 3 October 2024 / Accepted: 15 December 2024

Abstract The very high luminosity run foreseen at the Z-pole for the FCC-ee will allow the detection in Z decays of new particles with very low couplings to the Standard Model. These particles can have measurable flight paths before they decay. If the timing and the position of the decay vertex can be measured with high precision, the mass of such particles can be measured by exploiting the constrained kinematics of an e^+e^- collider. The mass resolution achievable with this technique is studied through a detailed analysis in the framework of a parametrised simulation of the performance of the IDEA detector. The adopted benchmark model is the production of Heavy Neutral Leptons, which is one of the key channels for new physics discovery at the FCC-ee.

1 Introduction

The next generation of proposed e^+e^- circular colliders, such as the CERN FCC-ee [1] will provide access to a broad range of physics studies, from precision measurements of the Higgs boson and of Standard Model (SM) parameters, to direct searches for physics beyond the Standard Model (BSM).

Among the most promising BSM signatures at FCC-ee are long-lived particles (LLPs), i.e. particles which decay inside the detector with a measurable path. The detection of such particles poses severe performance constraints on the detector design, and a recent review of studies in this sector can be found in [2].

As mentioned in [2], the mass of LLPs can be measured by combining the length and time of their decay in the detector with the kinematic beam constraints of FCC-ee. This possibility has been recognized for a considerable time, but the need for a large tracking volume, as well as a timing resolution in the ballpark of a few tens of picoseconds has so far placed the practical realisation of this idea out of experimental reach. These features are present in the proposed design for FCC potential detectors, and the present study formalizes and quantifies for the first time the expected performance of this measurement technique in the FCC-ee context.

The production of heavy neutral leptons (HNL) in the decay of the Z boson is used as a benchmark model, and the constraints on the experimental design are assessed on the basis of a parameterised simulation of the expected performance of the tracking system of the proposed IDEA detector.

The paper is organised as follows: the basic analytical formulas are first introduced and discussed. In the following section the benchmark physics model and the detector simulation setup are described. Finally the expected resolution on position and timing of the vertex are evaluated in this framework, yielding an assessment of the HNL mass measurement capabilites of the technique in the parameter space of the HNL model considered.

2 Mass measurement with vertex timing

Consider a long-lived neutral particle L of mass M_L which is produced at an e^+e^- collider with centre-of-mass energy E_{CM} recoiling against a known particle of mass M, and decays into ≥ 2 charged particles at a distance δd_L from the interaction point, with a delay δt_L from the time of the interaction. The momentum of L, p_L, is expressed in special relativity as:

$$p_L = M_L \gamma \beta \tag{1}$$

[a] e-mail: giacomo.polesello@cern.ch
[b] e-mail: nicolo.valle@cern.ch (corresponding author)

Published online: 09 January 2025

with $\beta = \delta d_L/\delta t_L/c$, with c the speed of light, and is constrained by the collision kinematics through the recoil relation:

$$p_L = \frac{\sqrt{(E_{CM}^2 - (M_L + M)^2)(E_{CM}^2 - (M_L - M)^2)}}{2E_{CM}} \quad (2)$$

By eliminating p_L, M_L can be measured as a function of β, M and E_{CM}, which are measurable or known quantities.

This study explores what kind of precision one can realistically obtain within the detector systems being designed for experimentation at FCC-ee. To this purpose we work out analytically how the mass measurement depends on the detector performance, for the case $M = 0$, corresponding to a LLP recoiling against a massless particle such as a neutrino. In this case the formula for M_L reduces to:

$$M_L = E_{CM}\sqrt{\frac{1-\beta}{1+\beta}} \equiv E_{CM}F(\beta) \quad (3)$$

Thus the mass of the long-lived particle can be extracted from the measurement of its β.

Before discussing the detector simulation, it is informative to consider the expected mass resolution for values of M_L, δd_L relevant to experimentation at FCC-ee.

To this end, the uncertainty in M_L is related to the uncertainty on β by the approximate formula:

$$\sigma(M_L) = E_{CM}\frac{1}{\sqrt{\frac{1-\beta}{1+\beta}}(1+\beta)^2}\sigma(\beta) \equiv E_{CM}F'(\beta)\sigma(\beta) \quad (4)$$

which is valid for sufficiently high values of m_L and δd_L, such that β is significantly smaller than one.

If the dominant uncertainty in the measurement of β is the uncertainty on the δt_L, $\sigma(\delta t_L)$, this can be rewritten as

$$\sigma(M_L) = \frac{E_{CM}\beta^2 F'(\beta)c\sigma(\delta t_L)}{\delta d_L} \quad (5)$$

The uncertainty on M_L as a function of the decay path is shown in Fig. 1 respectively on the top for different values of M_L and an assumed uncertainty on the timing of 40 ps, and on the bottom for $M_L = 40$ GeV and three different values of the uncertainty on timing.For long lifetimes, above ~ 1 m, mass measurements below the percent level can be achieved, and the precision strongly depends on M_L, being worse for lower values of the mass.

One should note that the distribution of the measured mass is not Gaussian, but skewed towards low values, and the amount of asymmetry is a function of δd_L and of the mass,

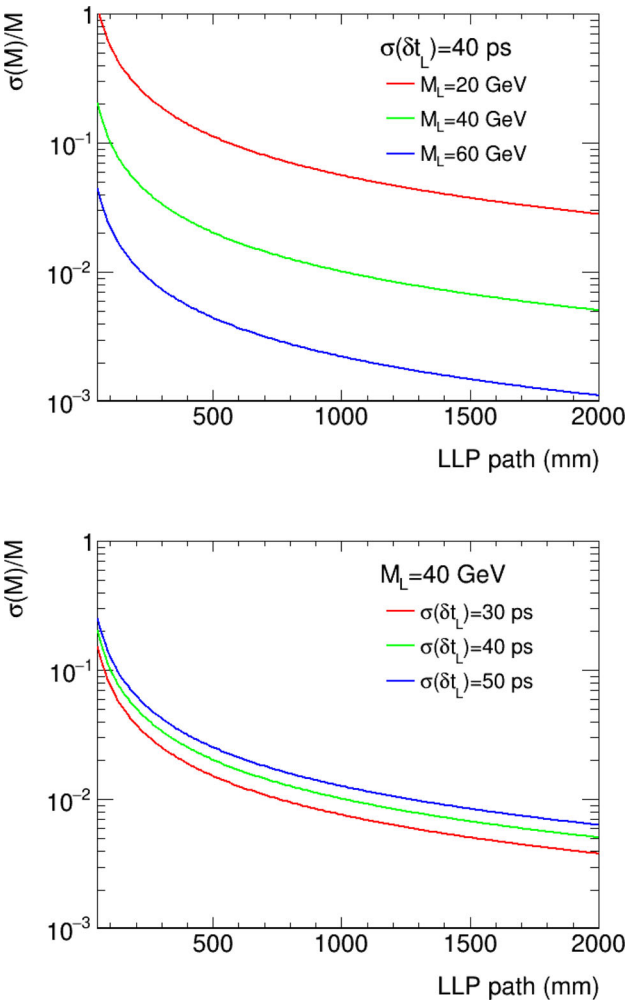

Fig. 1 Resolution of mass measurement through timing as a function of the LLP decay path. Top: for different values of M_L and an assumed uncertainty on the timing of 40 ps. Bottom: for $M_L = 40$ GeV and three different values of the uncertainty on timing

as shown on the top panel of Fig. 2,which depicts the distribution of the measured mass for a LLP of mass 30 GeV assuming a timing resolution of 40 ps for three different values of the LLP decay path: 10, 20, and 50 cm, obtained with a toy Monte Carlo generation. The dependence of this effect on the mass is shown on the bottom of Fig. 2, where the dependence of mass resolution from M_L, from Eq. 5 is compared to the offset on mass measurement when the value of the timing is moved by $\pm 1\sigma$ from the nominal value for $\delta d_L = 1$ m and $\sigma(\delta t_L) = 40$ ps. The Gaussian approximation is good for $M_L > 20$ GeV, but for M_L below 10 GeV the low-mass tails become dominant.

An additional interesting quantity is the minimum path length necessary for achieving a given value of $\sigma(M_L)$ as a function of M_L. This quantity determines the available statistics of measurable events as a function of the LLP lifetime. This is shown in Fig. 3 for $\sigma(\delta t_L) = 40$ ps, using as

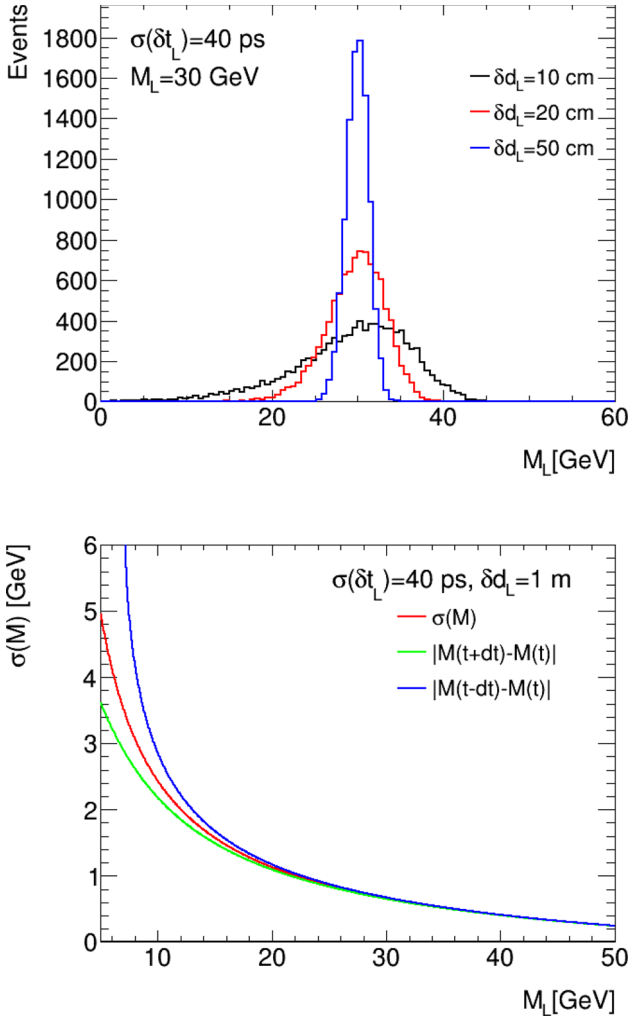

Fig. 2 Top: distribution of the measured mass for a LLP of mass 30 GeV assuming a timing resolution of 40 ps for three different values of the LLP decay path: 10, 20, and 50 cm. Bottom: mass resolution as a function of M_L as calculated with the error propagation (red line) compared to the offset on mass measurement when the value of the timing is moved by $\pm 1\sigma$ from the nominal value

a benchmark value a 20% resolution on the mass measurement. At low masses, below 20 GeV, only decays of the order of one meter yield a reasonable mass measurement, whereas for higher masses decays of a few centimetres are needed.

3 The simulation setup

In order to verify whether the technique described in Sect. 2 can work on a realistic BSM model we perform a study of the production of Heavy Neutral Leptons in the IDEA detector [3] at the FCC-ee. Generated signal events are passed through a parameterised simulation of the detector, and the parameter space of the model where the timing-based measurement can be applied is assessed.

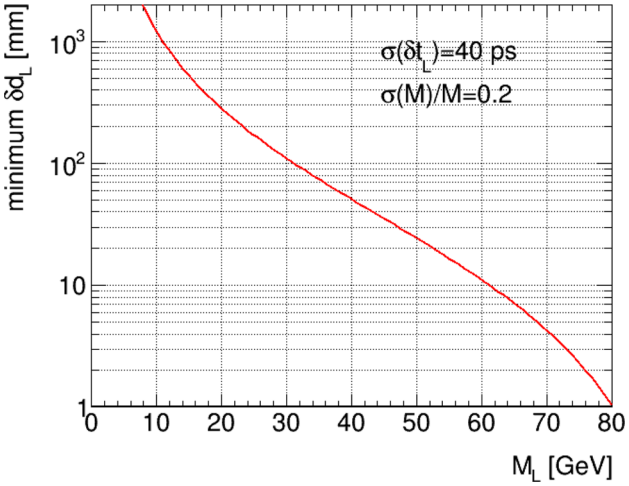

Fig. 3 Minimum decay length needed for achieving a 20% error on the mass measurement as a function of the mass of the LLP. The assumed resolution on timing is 40 ps

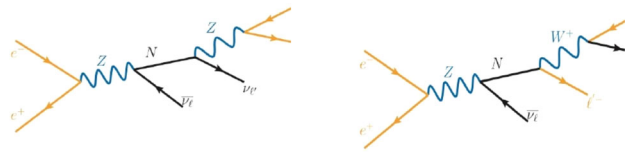

Fig. 4 Diagrams for production and decay of a heavy neutral lepton in the decay of a Z boson

3.1 Model definition and signal generation

The production of the HNL has been identified as one of the most promising new physics channels for FCC-ee at the Z pole in a seminal paper of 2014 [4], where details of the model can be found. The production of HNL in the decay of the Z bosons takes place through mixing with light neutrinos, yielding a HNL recoiling against a SM neutrino. The HNL decays into three fermions, through a virtual W or Z boson, as shown in Fig. 4.If only one HNL flavour is assumed, mixing only with one SM neutrino, the model is defined by two parameters: the HNL mass (M_{HNL}) and the mixing parameter U with the active neutrino. Long-lived (detached vertices) and prompt signatures are both possible depending on the the value of those parameters.

Several different decay channels and lifetime scenarios are accessible at the FCC-ee. Detailed discussions of previous experimental studies targeting FCC-ee are contained in [2,5]. As a benchmark for the present study the decay $HNL \rightarrow \mu jj$, is studied, which has a branching fraction of $\sim 50\%$. The simulated samples and the analysis code are the ones from the analysis documented in [6], where more details can be found.

The model of interest is implemented in the `SM_HeavyN_LO` [7–9] UFO, and signal samples were generated with

MG5aMC@NLO [10]. The masses of the heavy neutrinos N_2 and N_3 were set to 10 TeV, and all of the mixing terms were set to zero, except for the mixing between the muon and the HNL named as N_1 in the model. The associated production of a muon (anti)neutrino and the heavy neutrino N_1 was simulated, with the N_1 directly decayed into a muon and a quark-antiquark pair in the MG5 process card, so as to have the correct decay kinematics.

We performed a scan of the mass of N_1 between 5 and 85 GeV. For each mass, coupling values were simulated in a range going from the minimal coupling yielding at least one event decaying within 2.5 ms from the centre of the detector for the full FCC-ee Z-pole statistics, and a coupling squared of 5×10^{-4} which is excluded by existing experiments. The LHE files generated with MG5aMC@NLO are hadronised with PYTHIA8 [11] and then fed into the DELPHES [12] fast simulation of the IDEA Detector, based on the official data cards used for the "Winter2023" production of backgrounds [13].

For the backgrounds from Z decays, the official samples produced by the central software group for the FCC PED studies under the tag "Winter2023" were used [14]. The irreducible background from the four-fermion process $e^+e^- \to \mu\nu jj$ was produced at LO with MG5aMC@NLO, and passed through the same PYTHIA8-DELPHES chain as the signal events.

3.2 The IDEA detector and its simulation

The IDEA detector concept is a proposal for a general-purpose detector for the FCC-ee. The design includes an inner detector composed of 5 Monolithic silicon pixel (MAPS) layers followed by a high-transparency and high-resolution drift chamber. We assume the presence of a timing layer positioned around the inner tracker at an approximate radius of 2 ms from the interaction point. A silicon wrapper employing Resistive Silicon Detector technology has been proposed for this purpose to enhance the drift chamber's capabilities. This addition would effectively improve particle identification by providing precise spatial tracking along with timing measurements, achieving time resolutions on the order of tens of picoseconds, as documented in [15]. A superconducting solenoid producing a 2 T magnetic field surrounds the inner detector. Outside the solenoid is a high-resolution dual-readout fibre calorimeter, preceded by two preshower layers built with μ-rwell technology, and followed by three μ-rwell layers for muon detection, embedded in the return yoke of the solenoid.

The present analysis relies on the parameterised simulation in DELPHES of the inner detector for the estimate of the tracking and vertexing performance of IDEA. The vertex detector is simulated as 5 cylindrical layers with radius between 1.2 and 31.5 cm with 2-D readout, and resolution 3 μm except the outermost layer with a resolution of 7 μm, and 3 disks in each of the forward/backward regions with a resolution of 7 μm. The drift chamber is modelled as 112 co-axial layers, arranged in 24 identical azimuthal sectors, at alternating-sign stereo angles ranging from 50 to 250 mrad, and an assumed resolution on the single measurement of 100 μm. The chamber has a length of 4 ms, and covers the radius between 34 cm and 2 m, yielding full tracking efficiency for polar angles θ larger than about 10 degrees. The DELPHES simulation software relies on a full description of the geometry of the IDEA vertex detector and drift chamber and accounts for the finite detector resolution and for the multiple scattering in each tracker layer. It turns charged particles emitted within the angular acceptance of the tracker into five-parameter tracks (the helix parameters that describe the trajectory of the particle, including the transverse and longitudinal impact parameters), and determines the full covariance matrix of these parameters. Vertexes are reconstructed using these tracks as input, based on a simple χ^2 minimisation with constraints, yielding 3D vertexes with their χ^2 and covariance matrix. More details on the vertexing code used here can be found in [16].

4 Analysis and results

A full analysis based on the simulated samples for signal and background described in the previous section was performed. The analysis is focused on the run at the Z-pole, with an assumed statistics of 6×10^{12} produced Z bosons. The aim is to evaluate, for the benchmark model of HNL production, if there is a sizeable chunk of the parameter space where the timing-based mass measurement technique can be applied, and the expected resolution on the mass of the HNL. The detailed implementation of the analysis, and the resulting performance figures depend on the choice of the model. Therefore in the following the discussion of the analysis will refer to M_{HNL} rather than to the generic M_L introduced in Sect. 2.

A cartoon showing the projection of the relevant event topology in the plane transverse to the beam is shown in Fig. 5.

As explained in Sect. 2, in order to calculate M_L the quantities δd_L and δt_L need to be evaluated, with:

$$\delta d_L \equiv ||\overrightarrow{OV} - \overrightarrow{OI}|| \tag{6}$$

and

$$\delta t_L \equiv t_{vert} - t_{int}. \tag{7}$$

Here $\overrightarrow{OI}$ with magnitude d_{int} is the vector connecting the interaction vertex to the center of the detector, and t_{int} the

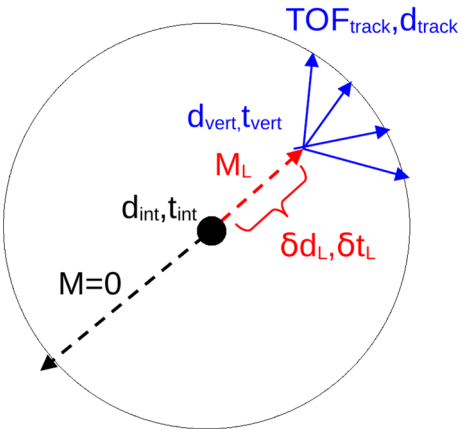

Fig. 5 Cartoon showing the different factors contributing to the measurement of the vertex timing

time difference between the interaction (primary) vertex and the zero time for the beam crossing. The equivalent quantities for the LLP decay (secondary) vertex are named $\overrightarrow{OV}$, d_{vert} and t_{vert}

Among these quantities, the three components of $\overrightarrow{OV}$, and hence their magnitude d_{vert} are measured directly in the tracking detector.

For each track attached to the decay vertex, three quantities can be measured: TOF_{track}, the arrival time of each charged particle to the timing layer situated around the outer radius of the IDEA tracker; the track momentum; and d_{track}, the length of the path of the track in the inner detector before reaching the timing layer.

The time t_{vert} is not directly measured, but it can be calculated on the basis of d_{vert} and of the measured track quantities through an algorithm which will be described in the following.

The experimental uncertainties on d_{vert}, d_{track} and momentum are determined by the design of the inner detector described above and are a function of the position of the decay vertex and of the number of tracks attached to it. The resolution on TOF_{track}, (σ(TOF)), does not depend on the topology of the event, and is determined by the technology chosen for the implementation of the tracking layer.

The quantities t_{int} and d_{int} cannot be measured, as the primary interaction results in two invisible neutrinos, and are constrained by the parameters of the accelerator.

The expected experimental uncertainties on the various quantities of interest are discussed in the following sections. The results are then combined into the desired estimate of the uncertainty of the HNL mass measurement.

4.1 Uncertainty on interaction point

The e^+e^- interaction point is centered in the center of the detector, and its time is centered on the nominal beam crossing time, which are taken as values of d_{int} and t_{int} for the calculation of the decay path of the HNL.

Fig. 6 Cartoon showing how the spread in time/position of the interaction vertex is generated in the crossing of the electron and positron beams

The shape of the interaction point at the FCC-ee, can be approximated as a 4-dimensional Gaussian distribution, determined by the size and shapes of the particle bunches in the accelerator and by their crossing angle.

With the FCC-ee parameters used for the current study [17,18], the interaction vertex will have a spread $\sigma_x = 5.96\ \mu$m, $\sigma_y = 23.8$ nm, $\sigma_z = 0.397$ mm, $\sigma_t = 36.3$ ps. A cartoon showing how this spread arises is shown in Fig. 6.

This spread in time and position of the interaction point will thus contribute to the uncertainty on the measurement of the LLP path length in the detector.

An additional uncertainty is the jitter in the reference signal of beam crossing delivered by the machine to the experiment, and how reproducible the centering of the beam crossing is fill by fill. From the LHC experience [19], the intrinsic jitter of the signal generated by RF of the accelerator is order 2 ps, with an additional 2 ps from the transmission to the experiments. As regards the reproducibility of the bunch structure and position, it is expected that it will be very precisely measured using the large number of available Z decays. This small uncertainty is ignored in the following calculations.

4.2 Uncertainty on vertex timing

The timing layer, located around the circle shown in Fig. 5, measures the arrival time of the charged particles from the HNL decay to the outer radius of the inner detector (TOF_{track}). For each track attached to the decay vertex the value of t_{hit}, which is the estimate for the track of the value of t_{vert} is calculated with the following procedure:

- The origin of the track (the HNL vertex) and its momentum are known.
- The helicoidal trajectory in the magnetic field is known. From its intersection to the timing layer, the flight distance d_{track} of the track from its origin to the layer can be calculated.
- If the mass of the particle producing the track is known, from the momentum and the flight distance the time of

flight of the track from its origin to the timing layer can be calculated.
– Subtract this time of flight from TOF_{track}. This gives t_{hit}.

If one of the decay products of the HNL is a muon, one can apply this procedure to the muon alone, which is well identified by the muon detector. However, if additional particles are produced, and their time of flight can be measured reliably, the precision of the timing measurement can be improved by a factor $\sqrt{N}$ where N is the number of tracks used for the measurement.

The achievable resolution using all tracks was studied on a benchmark sample of $HNL \to \mu jj$ decays, for $M_{HNL} =$ 40 GeV and proper time $c\tau_{HNL} = 1$ m passed through the parameterised simulation of the IDEA inner detector described in the previous section. The value of $\sigma(\mathrm{TOF})$ is assumed to be 30 ps, based on the detector design described in Sect. 3.2. If for each track the correct mass from Monte Carlo truth is assumed, the resolution on the timing is Gaussian, with an RMS of 11.2 ps, as shown in the black curves of the two distributions
shown in Fig. 7. This is approximately consistent with a $1/\sqrt{\langle N_{tracks}\rangle}$ scaling of the resolution, as the average number of tracks attached to the vertex is $\langle N_{tracks}\rangle = 8.2$.

A first approximation is to assign the pion mass to all of the tracks. The resulting timing resolution is shown as a blue line in the plots in Fig. 7. A very large tail in the timing resolution appears, badly spoiling the measurement.

The IDEA drift chamber has been designed to have a particle identification through cluster counting along a track, so it could be used to choose a mass hypothesis. However, for long HNL flight distances, the tracks are short, and it was found that the momentum of tracks peaks is in the region where particle separation by ionisation is not very powerful.

Therefore for the present exploratory exercise, a simple iterative algorithm based only on the TOF of the particles was developed:

– Use only tracks with $p_T > 300$ MeV.
– First use the pion mass hypothesis for all tracks that are not muons or electrons.
– For each hadron track, determine $\Delta t = |t_{hit} - Ave_{other}|$ where Ave_{other} is the average of of all other tracks. Find the track with the largest Δt.
– If $\Delta t >$ cut (set to 3×36 ps at the Z peak), try instead the kaon and proton hypotheses and keep the one that minimizes Δt.
– Iterate: find again the track with the worst Δt (the partial averages are recomputed), excluding the one found previously, up to the point where no improvement on Δt is possible.
– The average of all values of t_{hit} after the procedure is taken as the measurement of t_{vert}.

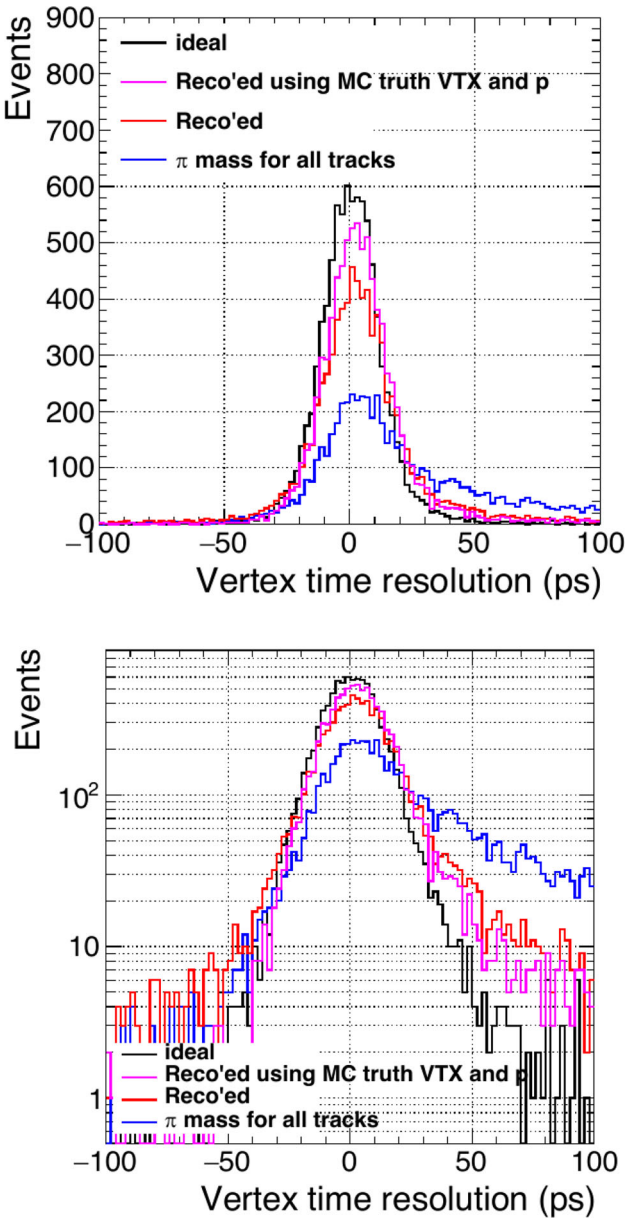

Fig. 7 Distribution of measured vertex timing for $M_{HNL} = 40$ GeV, $c\tau_{HNL} = 1$ m, $\sigma(\mathrm{TOF}) = 30$ ps. The different lines correspond to different approximations for the measurement. as described in the text. Top: linear scale; Bottom: logarithmic scale to better appreciate the tails for wrong assignment of the masses of decay products

The result of this algorithm is shown as a red line in Fig. 7. The tails are strongly reduced, although not fully eliminated. If a Gaussian fit is applied, the resolution is only 25% worse than in the ideal case. To understand the origin of the worsening in resolution, the algorithm was rerun using the 'truth' Monte Carlo position of the HNL vertex and momenta of the tracks. The result is shown as a magenta line, and shows that a large part of the worsening is not from the algorithm, but from the position and energy resolution of the detector.

Table 1 Vertex timing resolution for different values of M_{HNL} and $c\tau_{HNL}$. Ideal is the resolution in ps obtained using the correct mass assignment for tracks from the vertex and Reco'ed is the resolution using the algorithm described in the text. The average momentum and multiplicity of tracks from the vertex are also shown

M_{HNL} (GeV)	$c\tau_{HNL}$ (mm)	Ideal (ps)	Reco (ps)	$\langle p \rangle$ (GeV)	$\langle N_{tracks} \rangle$
10	1000	16.8	20.4	6.25	4.3
20	32	13.8	19.2	5.02	5.9
20	100	13.8	18.6	4.95	6.1
20	1000	14.4	21.0	4.87	5.9
20	3200	13.8	19.8	4.85	5.8
40	10	12.6	20.4	4.1	8.4
40	100	12.0	18.0	4.1	8.5
40	1000	12.6	22.8	4.02	8.2
60	10	11.4	21.6	3.84	10.4

In Table 1 the values of the vertex timing resolution for $\sigma(\text{TOF}) = 30$ ps are shown for different values of M_{HNL} and $c\tau_{HNL}$.

4.3 Uncertainty on vertex position

Based on the parameterised simulation of the inner detector performance, the resolution of the measured distance of the vertex from to the centre of the detector d_{vert} was evaluated for a sample of events with $M_{HNL} = 40$ GeV as a function of the value of d_{vert}, and is shown as black points in the top panel of Fig. 8. The resolution is approximately at a value of $\sim 100\,\mu$m when the vertex is fully in the drift chambers, and it improves as the vertex approaches the beam pipe thanks to the higher resolution of vertex detector. The relevant quantity for the mass measurement is however the HNL flight path, the distance from the unknown interaction point. The sigma of the distribution of the difference between d_{vert} and the HNL flight path is shown as red points in Fig. 8 for the same HNL sample, and it is approximately flat over the whole measurement range at a value between 200 and 250 μm.

In order to get a feeling of the relative importance of the uncertainty on position and timing of the vertex on the measurement of mass, the mass resolution was calculated assuming the timing perfectly measured (red points in the bottom panel of Fig. 8), and based on analytical formulas for a total timing resolution of 40 ps, incorporating both $\sigma(\text{TOF})$ and the 36.3 ps uncertainty on the interaction time (black points). The impact of the timing resolution is more than an order of magnitude larger than the one of position resolution.

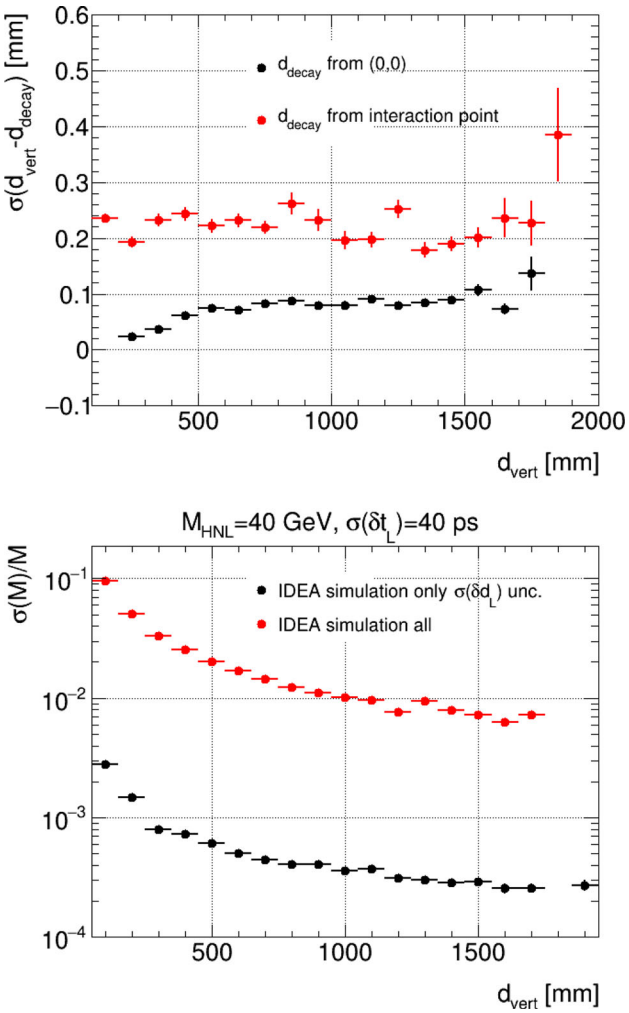

Fig. 8 Top: resolution on the position of the reconstructed vertex in the detector as a function of its position. Black points: intrinsic resolution of the vertex measurement. Red points: incorporate uncertainty on interaction point. Bottom: relative resolution on HNL mass measurement as a function of the position of the decay vertex. Black points: only uncertainty on vertex position considered. Red points: both uncertainty on timing and position considered. The assumed value of M_{HNL} is 40 GeV, and a total timing uncertainty of 40 ps is assumed

4.4 Uncertainty on mass as a function of flight path

Finally, the value of the HNL mass was calculated event-by-event on the basis of Formula 3, where β is calculated using the timing of the vertex calculated with the TOF measurement, and the distance d_{vert} is calculated from the vertex position measured by the inner detector. The two plots in Fig. 9 show the distribution of the difference between the

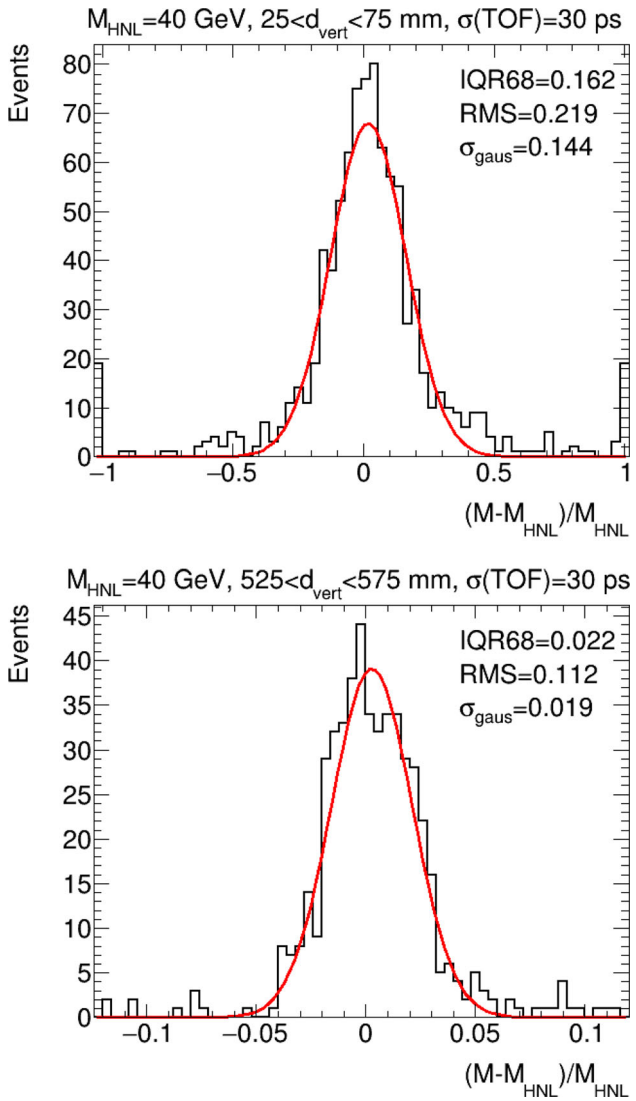

Fig. 9 Relative difference between the measured mass M and the nominal HNL mass m_{HNL} for two different bins in the vertex position d_{vert}. Assumed TOF uncertainty of 30 ps and $M_{HNL} = 40$ GeV

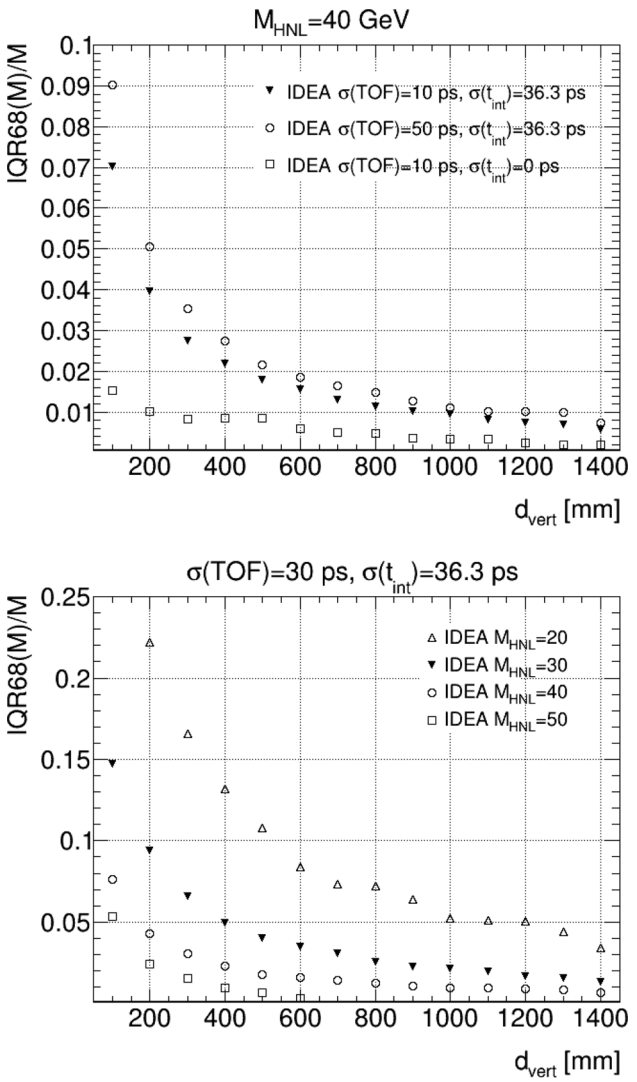

Fig. 10 Resolution of mass measurement through timing as a function of the position of the decay vertex. Top: $M_{HNL} = 40$ GeV and three different configurations for timing resolution; Bottom: σ(TOF) $= 30$ ps, and four values of M_{HNL}

measured mass M and the nominal $M_{HNL} = 40$ GeV scaled by M_{HNL} for σ(TOF) $= 30$ ps and two bins in d_{vert}, centered around respectively 50 and 550 mm. The two distributions show non-Gaussian tails on both sides, yielding a sigma of the Gaussian fit significantly better than the RMS of the distribution. As an estimator of the quality of the mass measurement the quantity IQR68 is defined, which is the interval between the quantile 16% and the quantile 84% of the mass distribution.

The distribution of the value IQR68/M as a function of d_{vert} is shown in Fig. 10. The top panel shows the resolution for $M_{HNL} = 40$ GeV, and two different values of σ(TOF), 10 and 50 ps respectively. The resolution in the 50 ps case is only 20% worse than in the 10 ps case, because the measurement is dominated by the lack of knowledge on the time of the interaction vertex. It can be concluded that value of σ(TOF) starts having a significant impact on the measurement starting from σ(TOF) ~ 50 ps.

Above $d_{vert} = 200$ mm the HNL mass is measured to better than 5%, going below 1% for $d_{vert} = 1500$ mm. As a comparison, the resolution is shown as well for the unphysical case where the timing of the interaction vertex is perfectly measured and σ(TOF) $= 10$ ps. In this case the mass would be measured to better than 1% starting from $d_{vert} = 200$ mm.

In the bottom panel the same resolution is shown for σ(TOF) $= 30$ ps and four different values of M_{HNL}. As expected, the resolution improves sharply when M_{HNL} increases.

4.5 Parameter space coverage

The achievable resolution on the mass as a function of the mass and of the path of a HNL in the inner detector of IDEA has been evaluated in the previous sections. The next step is the evaluation, in the framework of the benchmark model described in Sect. 3, and for the projected run at the Z-pole at the FCC, of the parameter space for which it is possible to measure the HNL mass with the timing technique described above.

For each model point the expected number of events N_{sig} surviving the selections in the Z-pole FCC run can be estimated. The study is performed on sets of Monte Carlo events where the HNL decays semi-leptonically into a muon and two quarks, corresponding to approximately 50% of the HNL decays. The normalisation considers all of the visible decays of the HNL, corresponding to approximately 93% of the decays, as only a moderate dependence of the timing measurement on the specific decay channel is expected.

A set of Monte Carlo experiments can be performed by selecting randomly in the sample of Monte Carlo signal events a number of events distributed according to a Poissonian distribution around N_{sig}. For each Monte Carlo experiment, the variance on the mass measurement strongly varies with the primary vertex position d_{vert}, and it is inversely proportional to the square of d_{vert} as shown in Formula 5.

The HNL mass is thus calculated for each experiment as the inverse variance weighted average of the measured masses, where the square of d_{vert} is taken as weighting factor. The uncertainty on the timing-based mass measurement is taken as the RMS of the averages over a number of Monte Carlo experiments.

The final state of interest is isolated by selecting events with one and only one reconstructed muon, no other reconstructed lepton, at least four reconstructed tracks and missing momentum larger than 5 GeV.

In order to guarantee that the vertex position is well reconstructed, the χ^2/ndf of the reconstructed vertex is required to be smaller than 10, and that at most 5 of the reconstructed tracks in the event are not used for the vertex reconstruction. As discussed in [6], this selection strongly reduces the background from the tails of $Z \to b\bar{b}$ production. We also require that the transverse distance of the vertex from the centre of the detector is larger than 5 cm.

This last selection guarantees that the Standard Model backgrounds are reduced to a negligible level, and that the mass measurement is not overly biased by the tails towards low masses which appear when the decay path of the HNL is too short as discussed above. The expected uncertainty on mass measurement obtained with this procedure is shown in Fig. 11 in the (M_{HNL}, U^2) plane, for an assumed uncertainty on TOF measurement of 30 ps. No value is shown for model points for which N_{sig} is larger than the number of available

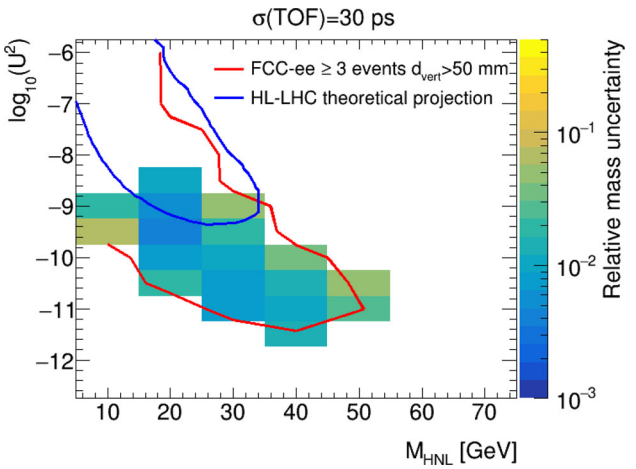

Fig. 11 Expected relative resolution on mass measurement as defined in the text, in the (M_{HNL}, U^2) plane for the Z-pole run of the FCC-ee. The red line bounds the region for which 3 events with $d_{vert} > 50$ mm survive the cuts. The blue line is a theoretical projection of the expected coverage in the same plane of HL-LHC searches. The assumed value of σ(TOF) is 30 ps

Monte Carlo signal events. The red line bounds the region where $N_{sig} \geq 3$. The optimistic expected coverage of HL-LHC based on a theoretical estimate [20] is shown as a blue line. Over all of the allowed region the HNL mass can be measured with the vertex timing technique discussed in this paper with a precision of a few percent. This measurement is independent from the measurement which can be obtained by measuring the visible mass in the detector using particle flow techniques combining information from the tracker and the calorimetric system. The final precision on the HNL mass will result from the combination of the two measurements.

5 Conclusions

The mass of a long-lived particle decaying within the FCC-ee detector can be determined by combining the timing and position of the decay vertex with constraints on beam energy and momentum. Using the relevant analytic formulas, it was shown that for timing resolutions of a few tens of picoseconds, a resolution on the mass of few percent for LLP mass in the range 10–80 GeV can be expected.

On the basis of a parametrised simulation of the IDEA detector, a complete analysis was performed for the production of an HNL in the process $Z \to \nu$HNL and its decay into a muon and two jets.

For time-of-flight measurements of HNL decay products in the range of 10–50 ps, the mass resolution is dominated by uncertainties in the timing and position of the initial interaction, undetectable and constrained solely by the geometry of the beam-beam collisions. For sufficiently long decay paths of the HNL, the analytical results are confirmed. A scan of

the parameters space of the HNL model, assuming the full statistics of the Z-pole run, shows that on a large part of the accessible space the experiments will be able to provide a measurement of the HNL mass with a precision of a few percent, based on the proposed technique.

Data Availability Statement This manuscript has associated data in a data repository. [Authors' comment: Part of the simulated Standard Model samples are produced by the central software group for the FCC PED studies and are available at https://fcc-physics-events.web.cern.ch/fcc-ee/delphes/winter2023/idea/.]

Code Availability Statement This manuscript has associated code/software in a data repository. [Authors' comment: The data cards for the DELPHES fast simulation of the IDEA Detector and the official FCC software are available at https://github.com/HEP-FCC/.]

Funded by SCOAP[3].

References

1. A. Abada et al., FCC-ee: the lepton collider: future circular collider conceptual design report volume 2. Eur. Phys. J. ST **228**(2), 261–623 (2019)
2. C.B. Verhaaren et al., Searches for long-lived particles at the future FCC-ee. Front. Phys. **10**, 967881 (2022)
3. M. Antonello, IDEA: a detector concept for future leptonic colliders. Nuovo Cim. C **43**(2–3), 27 (2020)
4. A. Blondel, E. Graverini, N. Serra, M. Shaposhnikov, Search for heavy right handed neutrinos at the FCC-ee. Nucl. Part. Phys. Proc. **273–275**, 1883–1890 (2016)
5. A.M. Abdullahi et al., The present and future status of heavy neutral leptons. J. Phys. G **50**(2), 020501 (2023)
6. G. Polesello, N. Valle, Sensitivity of the FCC-ee to decay of an HNL into a muon and two jets, FCC note (2023). https://doi.org/10.17181/9pc9x-kcn56
7. A. Atre, T. Han, S. Pascoli, B. Zhang, The search for heavy majorana neutrinos. JHEP **05**, 030 (2009)
8. D. Alva, T. Han, R. Ruiz, Heavy majorana neutrinos from $W\gamma$ fusion at hadron colliders. JHEP **02**, 072 (2015)
9. C. Degrande, O. Mattelaer, R. Ruiz, J. Turner, Fully-automated precision predictions for heavy neutrino production mechanisms at hadron colliders. Phys. Rev. D **94**(5), 053002 (2016)
10. J. Alwall, R. Frederix, S. Frixione, V. Hirschi, F. Maltoni, O. Mattelaer, H.S. Shao, T. Stelzer, P. Torrielli, M. Zaro, The automated computation of tree-level and next-to-leading order differential cross sections, and their matching to parton shower simulations. JHEP **07**, 079 (2014)
11. T. Sjöstrand, S. Ask, J.R. Christiansen, R. Corke, N. Desai, P. Ilten, S. Mrenna, S. Prestel, C.O. Rasmussen, P.Z. Skands, An introduction to PYTHIA 8.2. Comput. Phys. Commun. **191**, 159–177 (2015)
12. J. de Favereau, C. Delaere, P. Demin, A. Giammanco, V. Lemaître, A. Mertens, M. Selvaggi, DELPHES 3, a modular framework for fast simulation of a generic collider experiment. JHEP **02**, 057 (2014)
13. https://github.com/HEP-FCC/FCC-config/tree/winter2023/FCCee
14. https://fcc-physics-events.web.cern.ch/fcc-ee/delphes/winter2023/idea/
15. N. Cartiglia et al., Resistive read-out in thin silicon sensors with internal gain. JPS Conf. Proc. **42**, 011023 (2024)
16. F. Bedeschi, A vertex fitting package (2024). https://doi.org/10.48550/arXiv.2409.19326
17. F. Zimmermann, I. Agapov, Summary talk of Work Package 2, FCCIS 2022 Workshop (2022). https://indico.cern.ch/event/1203316/contributions/5177179/attachments/2563984/4420707/summaries_IA.pdf
18. FCC ee Physics Performance group, https://github.com/HEP-FCC/FCCeePhysicsPerformance/tree/master/General
19. S. Baron, T. Mastoridis, J. Troska, P. Baudrenghien, Jitter impact on clock distribution in LHC experiments. JINST **7**, C12023 (2012)
20. M. Drewes, J. Hajer, Heavy neutrinos in displaced vertex searches at the LHC and HL-LHC. JHEP **02**, 070 (2020)